Raman scattering from $YBa_2Fe_3O_{8+\delta}$

Y. K. Atanassova and V. G. Hadjiev
Department of Physics, University of Sofia, BG-1126, Sofia, Bulgaria

P. Karen and A. Kjekshus
Department of Chemistry, University of Oslo, Blindern, N-0315 Oslo, Norway
(Received 28 December 1993)

The results of polarized micro-Raman scattering experiments on $YBa_2Fe_3O_{8+\delta}$ with $\delta = 0.1$ are reported. We identified seven out of the total ten by symmetry Raman-allowed phonons at 134 cm^{-1} (A_{1g}), 148 cm^{-1} (E_g), 219 cm^{-1} (A_{1g}), 300 cm^{-1} (B_{1g}), 478 cm^{-1} (A_{1g}), 493 cm^{-1} (E_g), and 691 cm^{-1} (A_{1g}). The Raman-active phonons are assigned to definite atomic vibrations in close comparison with the structurally similar $YBa_2Cu_3O_6$, using simple considerations based on charge and bond length.

The Fe doping of $YBa_2Cu_3O_{7-\delta'}$ has been extensively applied because of the tendency of Fe^{3+} to take a higher oxygen coordination than Cu^{2+} (resulting in structural changes in the basal plane[1]) and owing to the convenience of Fe isotopes as probes to explore the oxygen surroundings by Mössbauer spectroscopy.[2] Although samples of $YBa_2Cu_3O_{7-\delta'}$ with Fe partially (up to 20%) substituted for Cu have been available for some time, a complete substitution of Cu resulting in single phase $YBa_2Fe_3O_{8+\delta}$ samples has not been reported until recently.[3–5] Along with the structural[4,6,7] and magnetic properties[5–8] of this compound, an experimental study of the phonon modes in $YBa_2Fe_3O_{8+\delta}$ (structurally similar to $YBa_2Cu_3O_{7-\delta'}$) is interesting not only in its own right, but also for a better understanding of the interplay between the composition, structure, and superconductivity.

In this Brief Report we present the results of polarized Raman spectroscopy of $YBa_2Fe_3O_{8.1}$. We also show that a simple model valid for a harmonic ionic crystal describes fairly well the changes of the measured phonon frequencies on going from $YBa_2Cu_3O_6$ to $YBa_2Fe_3O_8$.

In our experiments, we recorded the Raman spectra of individual crystals constituting a pellet of a sample with composition $YBa_2Fe_3O_{8.1}$, synthesized as described in Ref. 5. The visual observation through an optical microscope of the polished surface of the samples under polarized light revealed differently oriented, mostly elongated microcrystal projections of about 5 μm × 15 μm. We found that similarly to $YBa_2Cu_3O_{7-\delta'}$, the microcrystals of $YBa_2Fe_3O_{8.1}$ had grown as platelets with large faces parallel to the *ab* planes (*a*, *b*, and *c* being the crystallographic axes). Therefore, the long sides of the elongated projections were along a direction defined as *x* in the *ab* planes. The direction that is perpendicular to *x* (hereafter denoted *z*) lies in a plane that includes the *c* axis. As long as the *ab* plane is the plane of easy cleavage, it is exhibited by most of the grains on the surface of a freshly broken pellet.

The Raman spectra were measured[9] in backward scattering geometry from microcrystals exhibiting *xz* and *ab* surface orientations. We relate the scattering configurations either to the *x*, *y*, and *z* system or to the crystallographic axes. The latter is applied for those specimens where the crystallographic directions were unambiguously identified. The laser power density ($\lambda_L = 488$ nm), focused on a spot of diameter ~2 μm, was typically of 150 W/cm^2. Under these conditions, no visible changes of the exposed surface were observed.

The structure of $YBa_2Fe_3O_8$ Ref. (4) (see Fig. 1) is very similar to that of $YBa_2Cu_3O_6$.[10] The Y, Ba, Fe(1), Fe(2), and relevant oxygen atoms occupy sites of the same symmetry as those in $YBa_2Cu_3O_6$, and the numbering of the atoms also matches; e.g., Fe(1) and Fe(2) in $YBa_2Fe_3O_8$ occupy sites corresponding to Cu(1) and Cu(2) in $YBa_2Cu_3O_6$, respectively. The only notable

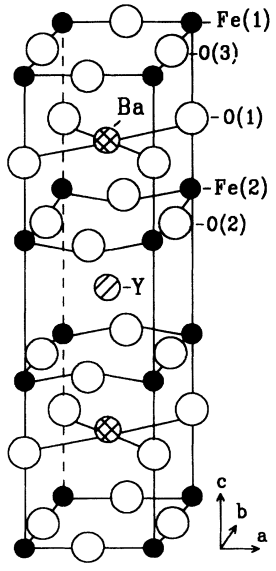

FIG. 1. The crystal structure of $YBa_2Fe_3O_8$ (space group $P4/mmm$). Relevant interatomic distances (in Å) from Ref. 4: Fe(1)–O(1) 2.134, Fe(2)–O(1) 1.872, Fe(2)–O(2) 2.014, Ba–O(1) 2.775, Ba–O(2) 3.190, Ba–O(3) 2.768, Y–O(2) 2.430, O(1)–O(2) 3.052, O(1)–O(3) 2.896. Corresponding distances in $YBa_2Cu_3O_6$ from Ref. 10: Cu(1)–O(1) 1.801, Cu(2)–O(1) 2.466, Cu(2)–O(2) 1.942, Ba–O(1) 2.774, Ba–O(2) 2.918, Y–O(2) 2.396, O(1)–O(2) 3.297.

TABLE I. Wyckoff notations, site symmetries and the irreducible representations for the atoms in $YBa_2Fe_3O_8$, space group $P4/mmm$.

Atom	Wyckoff notation	Site symmetry	Irreducible representation
Y	1(d)	$4/mmm$	$A_{2u}+E_u$
Ba	2(h)	$4mm$	$A_{1g}+A_{2u}+E_g+E_u$
Fe(1)	1(a)	$4/mmm$	$A_{2u}+E_u$
Fe(2)	2(g)	$4mm$	$A_{1g}+A_{2u}+E_g+E_u$
O(1)	2(g)	$4mm$	$A_{1g}+A_{2u}+E_g+E_u$
O(2)	4(i)	$2mm$	$A_{1g}+A_{2u}+B_{1g}+B_{2u}+2E_g+2E_u$
O(3)	2(f)	mmm	$A_{2u}+B_{2u}+2E_u$

Modes classification

$\Gamma_{\text{Raman}} = 4A_{1g} + B_{1g} + 5E_g$
$A_{1g} \rightarrow \alpha_{xx} + \alpha_{yy}, \alpha_{zz}$
$B_{1g} \rightarrow \alpha_{xx} - \alpha_{yy}$
$E_g \rightarrow \alpha_{xz}, \alpha_{yz}$

$\Gamma_{\text{ir}} = 6A_{2u} + 8E_u$
$\Gamma_{\text{silent}} = 2B_{2u}$
$\Gamma_{\text{acoustic}} = A_{2u} + E_u$

difference between the two structures originates from the difference in oxygen content and amounts to a full occupancy of the oxygen positions in the basal plane [containing the Fe(1)] of $YBa_2Fe_3O_{8+\delta}$. Given the symmetry of the atomic sites in $YBa_2Fe_3O_{8.1}$,[4,6,7] we performed a symmetry-group analysis using the method described in Ref. 11. The results are presented in Table I. Since the unit cell has a center of inversion, there are only ten Raman-active (even) modes $4A_{1g}$, B_{1g}, and $5E_g$, with the nonzero Raman tensor elements[11] given in Table I. The remaining (odd) vibrational modes are ir-active and the two B_{2u} modes are silent.

Figure 2 displays the polarized Raman spectra of $YBa_2Fe_3O_{8.1}$ microcrystals as measured in the most informative scattering configurations, viz., the $y(zz)\bar{y}$, $y(xx)\bar{y}$, $y(xz)\bar{y}$, $c(a+b,a+b)\bar{c}$, and $c(a+b,a-b)\bar{c}$, where $a+b$ and $a-b$ are two mutually perpendicular directions at an angle of 45° with respect to the $a(b)$ axis. The latter configuration allows unambiguous identification of the mode of B_{1g} symmetry ($\alpha_{xx} = -\alpha_{yy}, \alpha_{zz} = 0$). It follows from Fig. 2 that seven modes are clearly observed at 134 cm^{-1} (A_{1g}), 148 cm^{-1} (E_g), 219 cm^{-1} (A_{1g}), 300 cm^{-1} (B_{1g}), 478 cm^{-1} (A_{1g}), 493 cm^{-1} (E_g), and 691 cm^{-1} (A_{1g}). Their symmetries were identified using the selection rules given in Table I. The remaining three E_g modes which have to be present in the xz spectra are likely to be hidden by the polarization leakages from the strong A_{1g} and/or B_{1g} modes. These leakages may be favored by a slightly imperfect alignment of the microcrystals under study. We failed to observe any Raman modes stemming from the extra oxygen in our samples. However, this is in line with the neutron power diffraction results for $YBa_2Fe_3O_{8+\delta}$ (Ref. 6) and $(Y_{1-x}Ca_x)Ba_2Fe_3O_{8+\delta}$,[7] which show that the extra oxygen ($\delta > 0$) occupies the 1(b) position in the unit cell. Since the 1(b) position has the same site symmetry as 1(a) and 1(d), it follows from Table I that atoms at 1(b) sites can participate only in odd, Raman-forbidden modes.

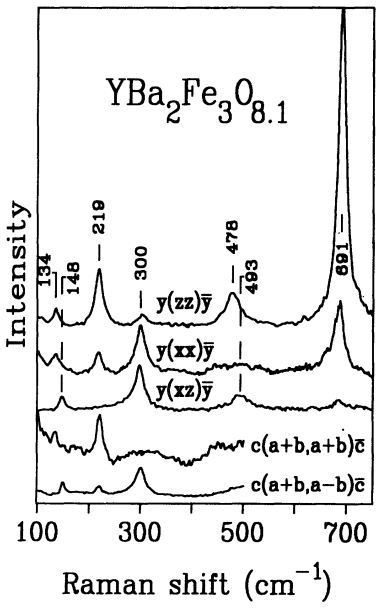

FIG. 2. Polarized Raman spectra of $YBa_2Fe_3O_{8.1}$ in the most informative $y(zz)\bar{y}$, $y(xx)\bar{y}$, $y(xz)\bar{y}$, $c(a+b,a+b)\bar{c}$, and $c(a+b,a-b)\bar{c}$ scattering configurations.

Generally, the Raman spectra in Fig. 2 resemble those of $YBa_2Cu_3O_{7-\delta'}$,[12] although there is a substantial increase in all phonon frequencies, except for that of the B_{1g} mode at 300 cm^{-1}. Further, a consistent explanation of the mode hardenings will be proposed based on ion-charge and bond-length considerations. We assume that the force constant k between the ions M and O follows a simple $Z_M Z_O / r^3_{M-O}$ relation where r_{M-O} is the cation-oxygen distance and Z_M and Z_O are the charge of the cation and oxygen, respectively. This relation is valid for a harmonic ionic crystal and shown to apply to various materials with the zinc-blende type structure for different degrees of covalence.[13] Such a simple model has been successfully used to explain the frequency variation of the apex oxygen O(1)-A_{1g} Raman mode with Sr substitution for Ba in $YBa_2Cu_3O_7$.[14] From Fig. 1 it follows that the directions of cation-oxygen bonds are either along the c axis or in the ab plane. Similarly to

$YBa_2Cu_3O_6$,[15] the eigenvectors of the Raman-active vibrations are parallel or perpendicular to a given cation-oxygen bond. Further, we assume that the restoring force that drives a displaced ion to equilibrium is mainly due to the change of the Coulomb part of its energy. For this particular case, it is easy to show that for a given bond, the force constants differ by a factor of 2 depending on whether the vibration is of the bond-stretching or bond-bending type: $k_{\text{stretching}} = 2k_{\text{bending}}$. Taking into account that $\omega^2 = k/m$, the frequency ratio for a *particular oxygen vibration* in $YBa_2Fe_3O_8$ (YBFO) and $YBa_2Cu_3O_6$ (YBCO) can be written as

$$\frac{\omega^2_{O-M}(\text{YBFO})}{\omega^2_{O-M'}(\text{YBCO})} = \frac{\sum pZ_M/r^3_{O-M} - \sum Z_O/r^3_{O-O}}{\sum pZ_{M'}/r^3_{O-M'} - \sum Z_O/r^3_{O-O}}, \quad (1)$$

where the sums in the first terms on the right side in both the numerator (YBFO) and denominator (YBCO) run over all nearest-neighbor cations. The oxygen repulsion from the next-nearest oxygen neighbors is also taken into account. In Eq. (1) the parameter p takes the value 2 or 1 depending on whether the vibration is of predominantly stretching or bending type with regard to the deformation of a particular bond. Note that one of the obvious reasons for the increase of ω_{O-M} comes from the higher valency 3+ of the Fe ions[4,7] in comparison with Cu. When the attention is shifted from oxygen to iron (copper), Eq. (1) has to be modified to account *inter alia* for the different mass of Fe and Cu, giving the relevant ratio of the Fe and Cu phonon frequencies for the two compounds:

$$\frac{\omega^2_{Fe-O}(\text{YBFO})}{\omega^2_{Cu-O}(\text{YBCO})} = \left(\frac{m_{Cu}}{m_{Fe}}\right)\frac{\sum pZ_{Fe}/r^3_{Fe-O}}{\sum pZ_{Cu}/r^3_{Cu-O}}. \quad (2)$$

Below we give the assignment of the observed Raman modes of $YBa_2Fe_3O_8$ (Table II) in more details.

(i) The strongest Raman peak appears at 691 cm^{-1} (Fig. 1), mostly zz polarized. We assign this peak to the apex oxygen O(1) stretching vibration along the Fe(1)−O(1)−Fe(2) bonds. The mode frequency is ~40 % higher than the corresponding mode in $YBa_2Cu_3O_{7-\delta'}$.[12] Similar hardenings of the apex-oxygen mode have also been observed for $RBa_2Cu_2NbO_8$ [R=Pr, La, or Nd (Ref. 16)] and $YBaCuFeO_5$,[9] where the mode appears at 689 and 669 cm^{-1}, respectively. These observations along with the existence of reliable experimental data on the interatomic distances in $YBa_2Fe_3O_8$ (Ref. 4) and $YBa_2Cu_3O_6$ (Ref. 10) (which are given in the caption to Fig. 1) stimulated us to analyze the apex-oxygen mode hardening with the model described by Eq. (1). In order to estimate the expected $\omega_{O(1)-Fe}$ frequency we have used the following experimentally determined oxygen-cation bond lengths: O(1)−Fe(1)/Cu(1) (one stretching), O(1)−Fe(2)/Cu(2) (one stretching), O(1)−Ba (two bending), and those of the oxygen neighbors O(1)−O(2) (four bending) and O(1)−O(3) (four bending bonds for YBFO). Further, taking into account the appreciable difference in the valency of the cations in the two compounds [$Cu(1)^{1+}$, $Cu(2)^{2+}$ for $YBa_2Cu_3O_6$ (Ref. 10), $Fe(1)^{3+}$, $Fe(2)^{3+}$ for $YBa_2Fe_3O_8$ (Refs. 4,7)] and $\omega_{O(1)-Cu}$ = 482 cm^{-1} for $YBa_2Cu_3O_6$,[12] Eq. (1) gives $\omega_{O(1)-Fe}$ = 695 cm^{-1}. It is remarkable that this rough approach only gives a 4 cm^{-1} deviation from the experimentally measured mode frequency.

TABLE II. Experimentally observed and calculated (see the text) Raman frequencies for $YBa_2Fe_3O_{8.1}$.

Atom	Mode	Obs.[a] ω_{YBCO}	Obs. ω_{YBFO}	Calc. ω_{YBFO}
O(1)	A_{1g}	482	691	695
	E_g	–	493	491
O(2)	A_{1g}	450	478	485
	B_{1g}	340	300	–
Fe(2)/Cu(2)	A_{1g}	142	219	200
	E_g	–	148	141
Ba	A_{1g}	122	134	147

[a]Reference 12.

(ii) The assignment of the E_g mode at 493 cm^{-1} to the O(1) bending vibration is straightforward. Since the E_g mode involves atomic vibrations in the ab plane, which in the case of the O(1) apex oxygen can be regarded as bending deformations of all relevant bonds, one can apply the following crude expression: $\omega_{O(1)}(E_g) = \omega_{O(1)}(A_{1g})/\sqrt{2}$. Hence, the O(1)-$E_g$ mode should appear at 491 cm^{-1} provided the calculated frequency of 695 cm^{-1} for the O(1)-A_{1g} mode is correct. Note that one cannot directly compare the E_g mode frequencies of $YBa_2Fe_3O_8$ with those of the related modes in $YBa_2Cu_3O_6$. Despite exhausting Raman data available for nondegenerate B_{2g}/B_{3g} modes in $YBa_2Cu_3O_7$,[17] there are to our knowledge no reports on the E_g modes in $YBa_2Cu_3O_6$.

(iii) We attribute the A_{1g} mode at 478 cm^{-1} to the O(2)+O(2) in-phase vibrations along the c axis. The corresponding mode in $YBa_2Cu_3O_6$ (Ref. 12) is at 450 cm^{-1}. In order to estimate the frequency expected for $YBa_2Fe_3O_8$ we use Eq. (1) with the following bonds: O(2)−Fe(2)/Cu(2) (two bending), O(2)−Y (one bending), O(2)−Ba (two bending), and O(2)−O(1) (one bending) for $YBa_2Fe_3O_8/YBa_2Cu_3O_6$. The thus obtained frequency $\omega_{O(2)-Fe}$ = 485 cm^{-1} is again in good agreement with the experimental value.

(iv) The mode at 300 cm^{-1} exhibits B_{1g} symmetry. Since only one Raman-active vibration is expected with such a symmetry (Table I) we assign this mode to the O(2)−O(2) out-of-phase vibrations along the c axis. Therefore, the B_{1g} mode frequency in $YBa_2Fe_3O_8$ is ~40 cm^{-1} lower than in $YBa_2Cu_3O_6$.[12] In $RBa_2Cu_3O_{7-\delta'}$ phases (R = rare-earth element) this mode has been found to depend strongly on the ionic radius of R and to a lesser extent on the oxygen content.[18] The B_{1g} mode has a too complex eigenvector for the estimation of the frequency with the simple model behind Eqs. (1) and (2). It is instructive, however, to correlate the changes with R of the relevant bond lengths in $RBa_2Cu_3O_{7-\delta'}$ (Ref. 19) and the variation of the B_{1g} frequency.[18] The frequency of the B_{1g} mode in $RBa_2Cu_3O_{7-\delta'}$ decreases monotonously with increasing ionic radius of R, from 335 cm^{-1} for $TmBa_2Cu_3O_7$ to

315 cm^{-1} for $NdBa_2Cu_3O_7$.[18] The most important distance for this mode is the average Cu(2)−O distance in the basal plane of the square pyramid, which increases from 1.935 Å to 1.959 Å for $TmBa_2Cu_3O_7$ and $NdBa_2Cu_3O_7$, respectively.[19] Similar behavior is exhibited by the average R−O distance which increases from 2.372 Å (Tm) to 2.462 Å (Nd). In contrast, the Cu(2)-O(1) distance decreases with R from 2.277 Å to 2.247 Å on going from Tm to Nd.[19] Comparing the corresponding interatomic distances in $YBa_2Cu_3O_6$ and $YBa_2Fe_3O_8$ we find similar tendencies: The $M(2)$−O(2) distance increases from 1.942 Å for M =Cu (Ref. 10) to 2.014 Å for M = Fe,[4] whereas the $M(2)$−O(1) distance decreases strongly from 2.466 Å (Cu) to 1.872 Å (Fe).

(v) The A_{1g} mode at 219 cm^{-1} is assigned to the Fe(2) vibration along the c axis. The corresponding mode of Cu(2) in $YBa_2Cu_3O_6$ has been observed at 142 cm^{-1}.[12] Fe(2) and Cu(2) have the same oxygen surroundings (fivefold pyramidal coordination). The Fe atoms in $YBaCuFeO_5$ occupy sites of the same symmetry as Fe(2) in $YBa_2Fe_3O_8$ and Cu(2) in $YBa_2Cu_3O_6$. The relevant Fe vibration in $YBaCuFeO_5$ occurs at 214 cm^{-1}.[9] Taking into account the most important bonds for the Fe/Cu vibration in $YBa_2Fe_3O_8$/ $YBa_2Cu_3O_6$, Fe(2)/Cu(2)−O(1) (one stretching), Fe(2)/Cu(2)−O(2) (four bending), Eq. (2) gives ω_{Fe} = 200 cm^{-1}. Thus, the observed increase in the Fe-A_{1g} frequency can be attributed to the combined effects of lower mass, higher valency, and shorter Fe(2)−O(1) distance in $YBa_2Fe_3O_8$ compared with the corresponding parameters in $YBa_2Cu_3O_6$.

(vi) The second mode of E_g symmetry at 148 cm^{-1} (Fig. 1) can unambiguously be assigned to the Fe(2)-E_g mode. Indeed, it follows from (v) that the most important distance for the Fe(2) vibration is Fe(2)−O(1). In the Fe(2)-A_{1g} mode, the iron motion can be regarded as both a stretching of Fe(2)−O(1) and a bending of the longer Fe(2)−O(2) bonds. In the Fe(2)-E_g mode, the vibration is of the bending type for all bonds. Thus one can derive $\omega_{Fe}(E_g)$ from $\omega_{Fe}(A_{1g})$ in the same way as in (ii), $\omega_{Fe}(E_g) = \omega_{Fe}(A_{1g})/\sqrt{2}$ =141 cm^{-1}, provided the calculated $\omega_{Fe}(A_{1g})$=200 cm^{-1}.

(vii) The remaining A_{1g} mode at 134 cm^{-1} can directly be attributed to Ba vibration along the c axis. The corresponding Ba mode in $YBa_2Cu_3O_6$ is at 122 cm^{-1}.[20] In $YBa_2Cu_3O_6$ barium is coordinated to 8 oxygens, whereas, in $YBa_2Fe_3O_8$, barium has 12 oxygen neighbors.[4] Merely for this reason one may expect an increase of the Ba mode frequency in $YBa_2Fe_3O_8$. Introducing the relevant bonds Ba−O(1) (four bending), Ba−O(2) (four bending), and Ba−O(3) (four bending for $YBa_2Fe_3O_8$) into the analog of Eq. (2) for the Ba mode (where the mass quotient is 1), one obtains ω_{Ba}(YBFO)=147 cm^{-1}, which is ~8% higher then the experimental value.

In conclusion, from polarized micro-Raman spectra of $YBa_2Fe_3O_8$ we have identified seven out of the total ten Raman-allowed phonons and assign them to definite atomic vibrations. A simple model based on charge and bond-lengths considerations turns out to give reasonably adequate description of the frequency changes on going from $YBa_2Cu_3O_6$ to $YBa_2Fe_3O_8$. The observed increase in frequencies for most of the modes in $YBa_2Fe_3O_8$ is found to originate mainly from the bond-length changes, the higher valency, and the lower mass of Fe.

Numerous stimulating discussions with M. Iliev are highly appreciated. This work was supported in part by the Bulgarian National Foundation for Science under Contract No. F1/91.

[1] Y. Xu, M. Suenaga, J. Tafto, R. L. Sabatini, A. R. Moodenbaugh, and P. Zolliker, Phys. Rev. B **39**, 6667 (1989).
[2] P. Boolchand and D. McDaniel, in *Studies on High-Temperature Superconductors*, edited by A. V. Narlikar (Nova Science, New York, 1990), Vol. 4, p. 143.
[3] P. Karen, P. H. Andersen, and A. Kjekshus, J. Solid State Chem. **101**, 48 (1992).
[4] Q. Huang, P. Karen, V. L. Karen, A. Kjekshus, J. W. Lynn, A. D. Mighell, N. Rosov, and A. Santoro, Phys. Rev. B **45**, 9611 (1992).
[5] P. Karen and A. Kjekshus, J. Solid State Chem. (to be published).
[6] Q. Huang, P. Karen, V. L. Karen, A. Kjekshus, J. W. Lynn, A. N. Mighell, I. N. Sora, N. Rosov, and A. Santoro (unpublished).
[7] I. N. Sora, Q. Huang, J. W. Lynn, N. Rosov, P. Karen, A. Kjekshus, V. L. Karen, A. N. Mighell, and A. Santoro, Phys. Rev. B **49**, 3465 (1994).
[8] I. Felner, I. Nowik, U. Yaron, O. Cohen, E. R. Bauminger, T. Kroener, and G. Czjzek (unpublished).
[9] Y. K. Atanassova, V. N. Popov, G. G. Bogachev, M. N. Iliev, C. Mitros, V. Psycharis, and M. Pissas, Phys. Rev. B **47**, 15201 (1993).
[10] M. F. Garbauskas, R. W. Green, R. H. Arendt, and J. S. Kasper, Inorg. Chem. **27**, 871 (1988).
[11] D. L. Rousseau, R. P. Bauman, and S. P. S. Porto, J. Raman Spectrosc. **10**, 253 (1981).
[12] V. G. Hadjiev, M. N. Iliev, and P. G. Vassilev, Physica C **153-155**, 290 (1988).
[13] R. M. Martin, Phys. Rev. B **1**, 4005 (1970).
[14] M. Kakihana, S.-G. Eriksson, L. Börjesson, L.-G. Johansson, C. Ström, and M. Käll, Phys. Rev. B **47**, 5359 (1993).
[15] F. E. Bates, Phys. Rev. B **39**, 322 (1989).
[16] M. Bennahmias J. C. O'Brien, H. B. Radousky, T. J. Goodwin, P. Klavins, J. M. Link, C. A. Smith, and R. N. Shelton, Phys. Rev. B **46**, 11986 (1992).
[17] K. F. McCarty, J. Z. Liu, R. N. Shelton, and H. B. Radousky, Phys. Rev. B **41**, 8792 (1992).
[18] H. J. Rosen, R. M. Macfarlane, E. M. Engler, V. Y. Lee, and R. D. Jakowitz, Phys. Rev. B **38**, 2460 (1988).
[19] M. Guillaume, P. Allenspach, J. Mesot, B. Roessli, U. Staub, P. Fischer, and A. Furrer, Z. Phys. B **90**, 13 (1993).
[20] G. Burns, F. H. Dacol, C. Feidl, and F. Holtzberg, Solid State Commun. **77**, 367 (1991).